Journal of Colloid and Interface Science 377 (2012) 322–327

Contents lists available at SciVerse ScienceDirect

Journal of Colloid and Interface Science

www.elsevier.com/locate/jcis

Fabrication of $Co(OH)_2$ coated Pt nanoparticles as an efficient catalyst for chemoselective hydrogenation of halonitrobenzenes

Haiyang Cheng [a,b], Xiangchun Meng [a], Qiang Wang [a], Jun Ming [a], Yancun Yu [a,b], Fengyu Zhao [a,b,*]

[a] State Key Laboratory of Electroanalytical Chemistry, Changchun Institute of Applied Chemistry, Chinese Academy of Sciences, Changchun 130022, People's Republic of China
[b] Laboratory of Green Chemistry and Process, Changchun Institute of Applied Chemistry, Chinese Academy of Sciences, Changchun 130022, People's Republic of China

ARTICLE INFO

Article history:
Received 17 December 2011
Accepted 1 March 2012
Available online 23 March 2012

Keywords:
Platinum nanoparticles
$Co(OH)_2$
Chemoselective hydrogenation
Halonitrobenzene
Haloaniline

ABSTRACT

$Co(OH)_2$ coated platinum nanoparticles $Pt/Co(OH)_2$ were prepared by microwave assistance and hydrothermal method, and the prepared samples were composed of Pt nanoparticles with an average size of 1.8 nm coated uniformly in the thin $Co(OH)_2$ leaves based on the results of X-ray diffraction, transmission electron microscopy, scanning electron microscopy and X-ray photoelectron spectroscopy. The $Pt/Co(OH)_2$ presented excellent catalytic performance in the chemoselective hydrogenation of halonitrobenzenes such as chloronitrobenzenes, bromonitrobenzene and iodonitrobenzene, and above 99.6% selectivity to haloanilines was achieved at complete conversion irrespective of the substrates used, even for iodonitrobenzene to which the dehalogenation is more easily to occur. $Co(OH)_2$ was confirmed to prohibit the dehalogenation effectively, and the $Pt/Co(OH)_2$ catalyst could be recycled for several times.

1. Introduction

Haloanilines (HANs) are important industrial intermediates in the synthesis of organic dyes, perfumes, herbicides, pesticides, preservatives, plant growth regulators, medicines and light sensitive or nonlinear optical materials [1,2], and these organic amines are mainly produced from the selective hydrogenation of the corresponding halonitrobenzenes (HNBs) (Scheme 1). Recently, some progresses have been achieved through designing the effective catalysts to prevent the dechlorination in the hydrogenation of chloronitrobenzenes (CNBs), and high selectivities to chloroanilines (CANs) were obtained in a success [3–18], whereas the studies on the hydrogenation of bromo- or iodo-nitrobenzenes (BNBs, INBs) are very limited up to now [19–21], since it is well known that the Br–C and I–C bonds are more susceptible to hydrogenolysis due to the weaker bonding energy compared with Cl–C bond, deriving from the larger atomic diameter and lower electronegativity of bromine and iodine. More recently, a partially reduced Pt/γ-Fe_2O_3 nanocomposite was reported to be effective in catalyzing the hydrogenation of BNBs and INBs; at the complete conversions, the selectivities to BANs and IANs reached 99.9% and 99.4%, respectively [19,20]. Moreover, a selectivity of 99.5% to *p*-IAN at 99.5% conversion of *p*-INB was obtained over 0.2% Pt/TiO_2 catalyst [21]. It was also reported that n-octylamine could act as inhibitor to the hydrogenolysis of carbon–halogen bond during the hydrogenation of halonitrobenzene [22]. However, to improve the selectivity of HANs is still a hot topic because the hydrogenolysis of carbon–halogen bond usually occurs easily and it can be accelerated by amino substitution in the aromatic rings [23].

Metal nanoparticles are usually highly active and selective catalysts. Pt, Rh, Ru, Pd and PtRu nanoparticles were successfully prepared, and the particle size could be well controlled via a polyol process in ethylene glycol containing NaOH [24–26]. However, during the chemical reaction, the naked nanoparticles are easy to aggregate, resulting in a decrease in the catalytic activity and selectivity. To solve this problem, metal nanoparticles were immobilized onto the supports such as carbon, metal oxides, molecular sieves and polymers. In this work, platinum nanoparticles were prepared by reducing H_2PtCl_6 with ethylene glycol under microwave irradiation, and then these formed Pt nanoparticles were coated with $Co(OH)_2$ by hydrothermal method. The formed $Pt/Co(OH)_2$ samples were well characterized by X-ray diffraction (XRD), transmission electron microscopy (TEM), scanning electron microscopy (SEM) and X-ray photoelectron spectroscopy (XPS). The catalytic performance of $Pt/Co(OH)_2$ was studied for the hydrogenation of CNBs, *p*-BNB and *m*-INB, and it presented high selectivities to HANs due to the dehalogenation of HANs was fully inhibited, in which the function of $Co(OH)_2$ has been discussed in detail.

2. Materials and methods

2.1. Materials

$H_2PtCl_6{\cdot}6H_2O$ and 5-wt.% Pt/C catalyst were purchased from WAKO and used as received. NaOH, $CoCl_2{\cdot}6H_2O$, ethylene glycol,

* Corresponding author at: State Key Laboratory of Electroanalytical Chemistry, Changchun Institute of Applied Chemistry, Chinese Academy of Sciences, Changchun 130022, People's Republic of China. Fax: +86 431 8526 2410.
E-mail address: zhaofy@ciac.jl.cn (F. Zhao).

0021-9797/$ - see front matter © 2012 Elsevier Inc. All rights reserved.
http://dx.doi.org/10.1016/j.jcis.2012.03.042

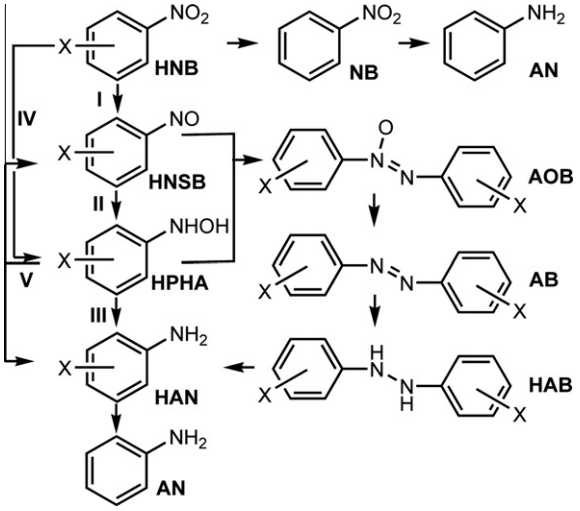

Scheme 1. Possible reaction pathway for the hydrogenation of halonitrobenzene. HNB: halonitrobenzene; HNSB: halonitrosobenzene; HPHA: halo-N-phenylhydroxylamine; HAN: haloaniline; NB: nitrobenzene; AN: aniline; AOB: azoxybenzene; AB: azobenzene; HAB: hydrazobenzene.

$NH_3{\cdot}H_2O$ (25.0–28.0 wt.% content of NH_3), ethanol and methanol are of analytical grade and used without further purification. Carbon black (VC72R, 254 m^2/g) was purchased from the Cabot Corporation; *o*-, *m*-, *p*-CNB, *p*-BNB and *m*-INB were purchased from Aldrich. Gases of N_2 (99.999%) and H_2 (99.999%) were purchased from Changchun Xinxing Gas Company and used as delivered.

2.2. Synthesis of platinum nanoparticles by microwave irradiation

$H_2PtCl_6{\cdot}6H_2O$ (0.0652 g) was dissolved in 6.5 ml of ethylene glycol containing 0.3 M NaOH. The solution was heated to 160 °C and stirred at 900 rpm for 3 min in microwave-assistant (Microwave synthesizer, Initiator, Biotage). In this manner, the Pt nanoparticles were formed in a dark brown solution.

2.3. Synthesis of cobalt hydroxide

In a typical preparation, 10 mmol $CoCl_2{\cdot}6H_2O$ was dissolved in 125 ml deionized water, and then excessive amounts of $NH_3{\cdot}H_2O$ were added dropwise into the above solution with vigorous stirring at room temperature until the pH value was adjusted to 10.0. After continuous stirring for 2 h, a large amount of cyan precipitate was obtained, and the pH of the solution did not change. The resulting precipitates ($Co(OH)_x$) were filtered and washed with deionized water, and then the fresh wet precipitate was re-dispersed in 35 ml deionized water, treated with ultrasonic for 1 h and moved into a 50 ml Teflon-lined stainless steel autoclave. The sealed autoclave was heated at 180 °C for 10 h and then cooled to room temperature. The resulting dust-color precipitates were filtered and washed with deionized water and pure ethanol, respectively, and finally dried in vacuum at 40 °C for 6 h.

2.4. Synthesis of cobalt hydroxide supported platinum catalyst

After the fresh $Co(OH)_x$ solution was treated with ultrasonic, the platinum nanoparticles prepared in ethylene glycol were added into the solution, and then the mixture was moved into 50 ml Teflon-lined stainless steel autoclave and hydrothermal treated at 180 °C for 10 h, followed by the cooling, washing and drying processes as described above.

2.5. Synthesis of 1% Pt/C catalyst

The platinum nanoparticles prepared in ethylene glycol (6.5 ml) were mixed with 2.4 g carbon black (XC-72R, 254 m^2/g), and additional 93.5 ml ethylene glycol was added. The obtained mixture was stirred at room temperature for 48 h and then filtered and washed with deionized water and ethanol, respectively, and lastly dried in vacuum at 40 °C for 12 h.

2.6. Catalyst characterization

Pt loading in the catalysts was measured by ICP-OES (iCAP6300, Thermo USA). The loading of Pt was 1% and 2.3% for Pt/C and Pt/$Co(OH)_2$, respectively. The metallic state on the surface of catalyst was examined by X-ray photoelectron spectroscopy (XPS, Thermo ESCALAB 250), and binding energies of the reference compounds and catalysts were measured using the C 1s peak (284.6 eV) of the adventitious carbon as an internal standard. For etching the surface layer, bombardment by argon ions with energy of 5000 eV was used, and the etching time was 5 min. X-ray diffraction (XRD) was performed with a D8 ADVANCE X-ray Diffractometer, and the scanning electron microscopy (SEM) was carried out on a Hitachi's S-4800 FE-SEM operating at 10.0 kV. Transmission electron microscopy (TEM) was performed using JEM-2010EX.

2.7. Hydrogenation of halonitrobenzenes

Catalytic experiments of chemoselective hydrogenation of halonitrobenzenes were carried out in a 50 ml autoclave equipped with magnetic stirring. In a typical hydrogenation process, 1 mmol substrate, 8.4 mg 2.3% Pt/$Co(OH)_2$ catalyst and 5 ml methanol were successively charged into the reactor. Then, the reactor was sealed and flushed three times with N_2 to remove the air. After flushing, the reactor was heated up to 60 °C. Hydrogen (2 MPa) was introduced, and then the reaction mixture was stirred for 30 min. After reaction, the liquid products were centrifuged and analyzed with a gas chromatograph (GC-Shimadzu-2010, FID, Capillary column, Rtx-5 30 m × 0.25 mm × 0.25 μm) and identified by gas chromatography/mass spectrometry (GC/MS, Agilent 5890). The GC results were obtained using an internal standard method, and *o*-xylene was always used as internal standard. For recycling experiment, the reaction mixture of the first run was centrifuged and separated by decantation, and then the solid catalyst was washed three times with solvent of methanol, and the next run was started with the fresh *o*-CNB and solvent.

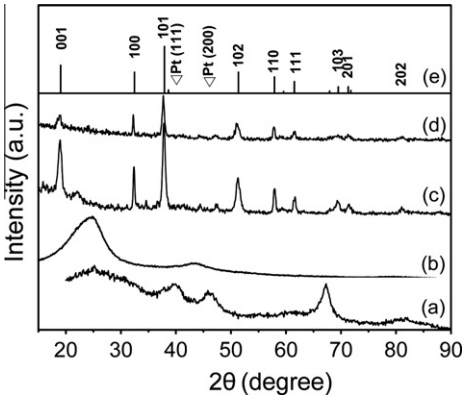

Fig. 1. X-ray diffraction patterns of (a) 5% Pt/C, (b) 1% Pt/C, (c) fresh Pt/$Co(OH)_2$ catalyst, (d) used Pt/$Co(OH)_2$ catalyst after the fifth reaction cycle and (e) JCPDS card No. 030-0443.

3. Results and discussion

3.1. Catalyst characterization

Fig. 1 shows the XRD pattern of the prepared Pt catalysts. For 1% Pt/C and Pt/$Co(OH)_2$, no evident characteristic diffraction peaks of Pt were detected, indicating that the Pt species in 1% Pt/C and Pt/$Co(OH)_2$ were highly dispersed and the particles were too small to detect (Fig. 1b–d), which will be demonstrated by the TEM results, while for 5% Pt/C, the Pt diffraction peaks were detected at 39.8° Pt (1 1 1) and 46.2° Pt (1 0 0), and the average size of Pt particle was about 4.5 nm based on the Debye–Scherer formula (Fig. 1a). Moreover, for the Pt/$Co(OH)_2$ samples, the diffraction peaks at about 19.00°, 32.42°, 37.78° and 51.28° are corresponding

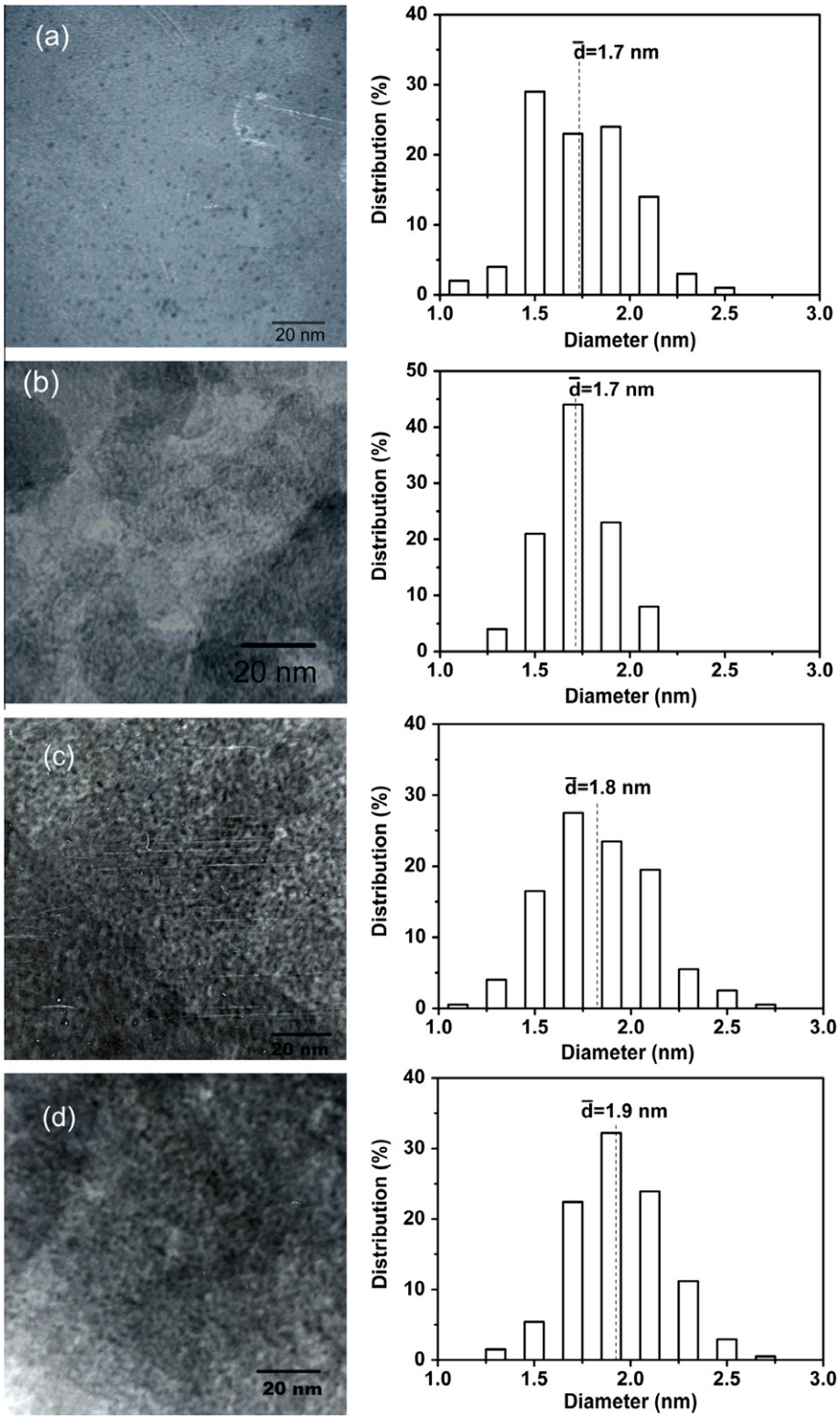

Fig. 2. TEM images and particle size distribution of (a) Pt nanoparticle, (b) 1% Pt/C, (c) fresh Pt/$Co(OH)_2$ catalyst and (d) used Pt/$Co(OH)_2$ catalyst after the fifth reaction cycle.

to (001), (100), (101) and (102) of $Co(OH)_2$ (Fig. 1c and d), and the XRD pattern matches the JCPDS 30-0443 file identifying $Co(OH)_2$ (Fig. 1e).

Fig. 2 shows the TEM images of the prepared Pt catalysts. It was obvious that the Pt nanoparticles formed under microwave irradiation in ethylene glycol had a narrow particle size distribution, and the average particle size is about 1.7 nm (Fig. 2a), and the particle size did not change anymore after they deposited onto the carbon, 1% Pt/C sample (1.7 nm in Fig. 2b). Furthermore, the loading of Pt on the prepared Pt/C was 1% from ICP analysis, which is the same to the theoretical value, indicating that Pt^{4+} was completely reduced to Pt^0 by ethylene glycol under microwave irradiation even in a short time (3 min). Ethylene glycol acts as a reducing agent; glycolate and oxalate formed by deprotonation of oxidation products (glycolic and oxalic acid) in alkaline solutions could interact with the Pt nanoparticles and hence act as their stabilizers possibly forming chelate-type complexes via its carboxyl groups [25]. For the fresh $Pt/Co(OH)_2$ catalyst, Pt nanoparticles were coated in $Co(OH)_2$ with a highly dispersion, and the average size of Pt particles is around 1.8 nm (Fig. 2c). The $Pt/Co(OH)_2$ samples presented a flowerlike morphology with many thin leaves from the SEM images, and the diameter of the $Pt/Co(OH)_2$ microspheres was distributed at a range of 5–20 μm (Fig. 3).

Fig. 4 shows the XPS spectra of Pt 4f peaks. For $Pt/Co(OH)_2$ sample, it did not present obvious peaks (Fig. 4a), but after the sample was argon ion etched for 5 min about 2–3 nm in depth, intense satellite peaks of Pt 4f appeared (Fig. 4b). This result strongly indicated that Pt nanoparticles were coated by $Co(OH)_2$. The binding energies of Pt $4f_{7/2}$ and Pt $4f_{5/2}$ of $Pt/Co(OH)_2$ were 70.94 and 74.62 eV, respectively, which are similar to the binding energies of PVP-protected Pt nanoparticles (70.99, 74.34 eV) [8], suggesting that all the Pt nanoparticles coated in $Co(OH)_2$ are metallic Pt rather than oxide Pt. The similar results were also obtained for 1% Pt/C (70.98, 74.33 eV) and 5% Pt/C (70.94, 74.50 eV) samples (Fig. 4c and d). The Co $2p_{3/2}$ peaks in the XPS spectra are shown in Fig. 5. From the spectra of XPS, the used catalyst did not found to be much different from the fresh one, and the intensive peaks at 780.5, 782.1 and 786.7 eV are belonged to the curve-fitted Co $2p_{3/2}$ spectra of $Co(OH)_2$, which are in agreement with the literature [27,28]. Based on the results of XRD and the XPS, the composition of support was confirmed to be $Co(OH)_2$ rather than CoO, Co_3O_4 or CoO(OH), and it was stable under the reaction conditions; no metallic Co was found on the surface of the recycled samples.

3.2. Catalytic performance of $Pt/Co(OH)_2$

The catalytic activity and selectivity of the $Pt/Co(OH)_2$ were examined for the hydrogenation of halonitrobenzenes such as *o*-CNB, *m*-CNB, *p*-CNB, *p*-BNB and *m*-INB, and the results are shown in Table 1. The $Pt/Co(OH)_2$ catalyst presented high selectivity irrespective of the reactants, and the selectivities to CANs were higher than 99.7% whatever extending the reaction time for the hydrogenation of *o*-, *m*- and *p*-CNB (entries 1–6). The high selectivity to *p*-BAN (99.7%) was also obtained in the hydrogenation of *p*-BNB at 100% conversion (entry 7). For *m*-INB, some intermediates such as diiodoazoxybenzene, diiodoazobenzene and diiodohydrazobenzene were produced initially and then transferred to the desired product of *m*-IAN (entries 9–11); the selectivity to *m*-IAN reached 99.6% at 100% conversion (entry 11). Moreover, with extending the reaction after 100% conversion achieved, the selectivity to deiodogenation product AN increased slightly due to the fact that the hydrogenolysis of the carbon–halogen bond can be accelerated by amino substitution in the aromatic rings once the substrate has been exhausted completely, but the selectivities to *p*-BAN and *m*-IAN were still above 99.1% (entries 8, 12). The above results indicated that the dehalogenation was fully inhibited over the present $Pt/Co(OH)_2$ catalyst. But for the Pt/C catalysts, large amount of deiodogenation product AN (>8%) was produced (entries 13–16), although 1% Pt/C catalyst has the similar particle size as

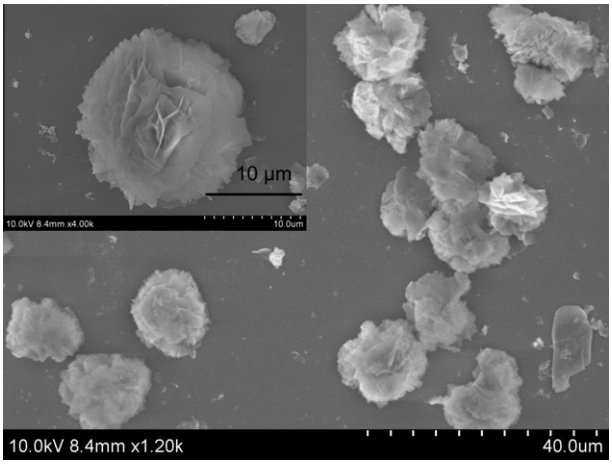

Fig. 3. FESEM images of $Pt/Co(OH)_2$.

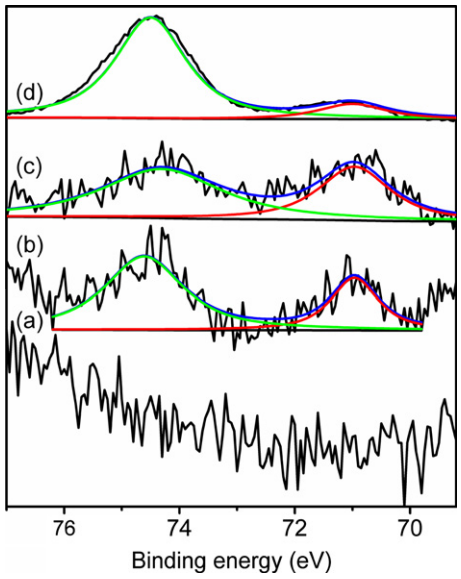

Fig. 4. XPS spectra of Pt in (a) fresh $Pt/Co(OH)_2$, (b) etching $Pt/Co(OH)_2$, (c) 1% Pt/C and (d) 5% Pt/C.

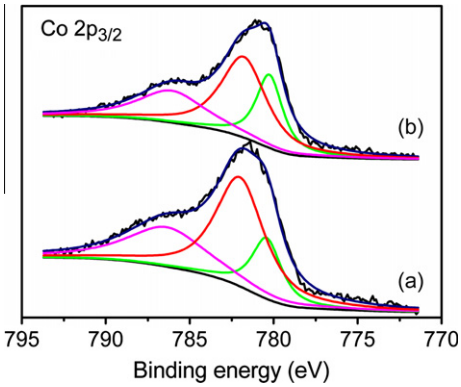

Fig. 5. XPS spectra of Co in (a) fresh $Pt/Co(OH)_2$ catalyst and (b) used $Pt/Co(OH)_2$ catalyst after the fifth reaction cycle.

Table 1
Results for the hydrogenation of halonitrobenzene over $Pt/Co(OH)_2$ and Pt/C catalysts at 60 °C.[a]

Entry	Reactant	Time (min)	Conv. (%)	Selectivity (%)		
				AN	HAN	Others[b]
2.3% $Pt/Co(OH)_2$						
1[c]	*o*-CNB	20	95.0	0.3	91.8	7.9
2[c]	*o*-CNB	120	100	0.3	99.7	–
3[c]	*m*-CNB	40	100	0.1	98.4	1.5
4[c]	*m*-CNB	120	100	0.1	99.7	0.2
5[c]	*p*-CNB	40	100	0.1	97.4	2.5
6[c]	*p*-CNB	120	100	0.2	99.7	0.1
7	*p*-BNB	30	100	0.3	99.7	–
8	*p*-BNB	60	100	0.7	99.3	–
9	*m*-INB	10	87.5	0.2	85.7	14.1
10	*m*-INB	20	100	0.3	97.6	2.1
11	*m*-INB	30	100	0.4	99.6	–
12	*m*-INB	120	100	0.9	99.1	–
5% Pt/C						
13	*m*-INB	30	100	4.9	93.7	1.4
14	*m*-INB	120	100	15.6	84.4	–
1% Pt/C						
15	*m*-INB	5	100	7.6	90.5	1.9
16	*m*-INB	120	100	8.2	91.8	–
1% Pt/C + $Co(OH)_2$[d]						
17	*m*-INB	2	58.1	2.2	83.3	14.5
18	*m*-INB	5	100	2.2	86.3	11.5
19	*m*-INB	15	100	2.7	97.3	–
$Co(OH)_2$						
20[d]	*m*-INB	120	2.9	–	49.5	50.5

[a] Reaction conditions: halonitrobenzene: 1 mmol, substrate/catalyst = 1000/1, methanol: 5 ml, H_2: 2 MPa. HAN is the haloanilines corresponding to the hydrogenated product of halonitrobenzene.
[b] Others products are by-products such as dihaloazoxybenzene, dihaloazobenzene and dihalohydrazobenzene.
[c] CNB: 5 mmol, substrate/catalyst = 5000/1.
[d] Twenty milligrams of $Co(OH)_2$ was used as additive.

that of $Pt/Co(OH)_2$. Therefore, it is the support which played very important role in controlling the product selectivity rather than the particle size. When the $Co(OH)_2$ and 1% Pt/C were used together, the deiodogenation was inhibited and the selectivity to *m*-IAN increased from 91.8% to 97.3% at the complete conversion of *m*-INB (entries 16, 19), although some intermediates increased during the reaction (entries 15, 18). For the present hydrogenation, however, the pure $Co(OH)_2$ showed very low activity (entry 20), and so, the presence of $Co(OH)_2$ was confirmed to be an inhibitor to the dehalogenation. Hydroxide as a catalytic support was reported in the literature [29,30]; recently, 99% selectivity to *o*-CAN was achieved at 99% conversion for the hydrogenation of *o*-CNB catalyzed with $Au/Fe(OH)_x$ catalyst [31], but lower activity was reported on $Pt/Fe(OH)_x$ catalyst in the presence of CO and H_2O [32]. Moreover, it was reported that $Mg(OH)_2$ and $Ca(OH)_2$ could suppress the dehalogenation in the hydrogenation of halonitroaromatics [33,34], which supported the present results. The activity of $Pt/Co(OH)_2$ was lower than that of Pt/C, owing to that Pt nanoparticles were immersed into the $Co(OH)_2$ thin leaves, and partial activity was weakened by the coated $Co(OH)_2$ layer with about 20 nm in thickness.

Strong metal–support interaction (SMSI) is an important factor for chemoselective hydrogenation of HNBs to HANs [4,8,19,20], and SMSI could be manifested by modifying the electron density of small clusters with charge transfer or polarization from partially reducible support [35], through the unique properties of metal–support borderline sites [36] and/or by decoration of the metal with mobile support [37]. The binding energies of Pt $4f_{7/2}$ and Pt $4f_{5/2}$ of Pt/C and $Pt/Co(OH)_2$ samples were the similar as that of PVP-protected Pt nanoparticles [8], suggesting that the SMSI in the $Pt/Co(OH)_2$ sample did not exist in present work.

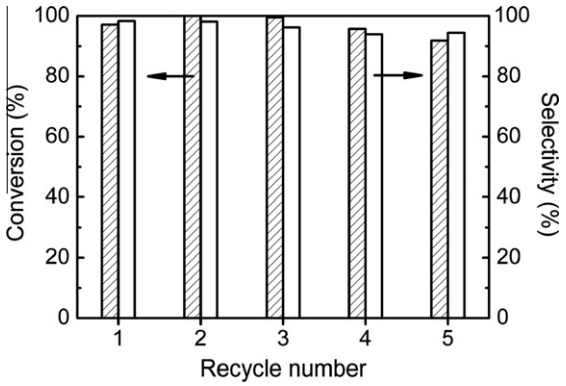

Fig. 6. The recycling results of $Pt/Co(OH)_2$ in the hydrogenation of *o*-CNB. Reaction conditions: *o*-CNB: 5 mmol, substrate/catalyst = 5000/1, *T*: 60 °C, methanol: 5 ml, H_2: 2 MPa, *t*: 30 min.

The stability of the $Pt/Co(OH)_2$ catalyst was checked, and the results are shown in Fig. 6. The catalyst presented to be relative stable under the reaction conditions, although a slight decrease in the conversion and selectivity appeared after the catalyst was reused for five times, but it still reached 92% and 94%, respectively. For the heterogeneous catalysis, metal species leaching usually occurs during the reaction, and is one problem for the supported catalysts separation and recycle. In this work, Pt leaching was not detected in the filtrate by ICP analysis (the detection limit was 0.1 ppm). Furthermore, TEM measurements showed that the Pt particles did not aggregate and the average size of Pt particles was still kept at about 1.9 nm (Fig. 2d) for the reused $Pt/Co(OH)_2$ sample, which was similar to that of the fresh one (1.8 nm) (Fig. 2c). These results should be ascribed to the special structure of the obtained $Pt/Co(OH)_2$ catalyst, in which all the Pt nanoparticles are coated by $Co(OH)_2$; thus, both the particle aggregation and the leaching of Pt were prevented successfully.

4. Conclusions

$Co(OH)_2$ coated platinum nanoparticles $Pt/Co(OH)_2$ have been successfully prepared in this work. The $Pt/Co(OH)_2$ presented a flowerlike morphology with many thin leaves, and the platinum nanoparticles were confirmed to be coated into the thin leaves of $Co(OH)_2$ with a high dispersity. Most importantly, the $Pt/Co(OH)_2$ showed high activity and selectivity for the hydrogenation of CNB, *p*-BNB and *m*-INB; above 99.6% selectivity to haloanilines was achieved at complete conversion irrespective of the reactants. These results were demonstrated to be benefited from the presence of $Co(OH)_2$ and its special structure. The presence of $Co(OH)_2$ successfully prevented the dehalogenation reactions and thus enhanced the selectivity of the desired product of haloanilines; the coated layer of $Co(OH)_2$ kept the Pt particles having a high dispersity and prohibited the aggregation of Pt particles as well as leaching of Pt species during the reaction. So that, the $Pt/Co(OH)_2$ catalyst showed good stability and could be recycled for several times.

Acknowledgment

This work was financially supported by NSFC 20873139, KJCX2, YW.H16 and 20111802.

References

[1] J.O. Morley, J. Phys. Chem. 99 (1995) 1923.

[2] Y. Okazaki, K. Yamashita, H. Ishii, M. Sudo, M. Tsuchitani, J. Appl. Toxicol. 23 (2003) 315.
[3] B.J. Zuo, Y. Wang, Q.L. Wang, J.L. Zhang, N.Z. Wu, L.D. Peng, L.L. Gui, X.D. Wang, R.M. Wang, D.P. Yu, J. Catal. 222 (2004) 493.
[4] J.L. Zhang, Y. Wang, H. Ji, Y.G. Wei, N.Z. Wu, B.J. Zuo, Q.L. Wang, J. Catal. 229 (2005) 114.
[5] Y.Y. Chen, C.A. Wang, H.Y. Liu, J.S. Qiu, X.H. Bao, Chem. Commun. (2005) 5298.
[6] Y.Y. Chen, J.S. Qiu, X.K. Wang, J.H. Xiu, J. Catal. 242 (2006) 227.
[7] L. Xing, J.S. Qiu, C.H. Liang, C. Wang, L. Mao, J. Catal. 250 (2007) 369.
[8] F. Wang, J. Liu, X. Xu, Chem. Commun. (2008) 2040.
[9] J. Xiong, J.X. Chen, J.Y. Zhang, Catal. Commun. 8 (2007) 345.
[10] F. Cardenas-Lizana, S. Gomez-Quero, M.A. Keane, Catal. Commun. 9 (2008) 475.
[11] F. Cardenas-Lizana, S. Gomez-Quero, M.A. Keane, Appl. Catal., A 334 (2008) 199.
[12] F. Cardenas-Lizana, S. Gomez-Quero, M.A. Keane, ChemSusChem 1 (2008) 215.
[13] N. Mahata, A.F. Cunha, J.J.M. Orfao, J.L. Figueiredo, Catal. Commun. 10 (2009) 1203.
[14] A. Corma, C. Gonzalez-Arellano, M. Iglesias, F. Sanchez, Appl. Catal., A 356 (2009) 99.
[15] H.Y. Cheng, C.Y. Xi, X.C. Meng, Y.F. Hao, Y.C. Yu, F.Y. Zhao, J. Colloid Interface Sci. 336 (2009) 675.
[16] X.C. Meng, H.Y. Cheng, S. Fujita, Y.F. Hao, Y.J. Shang, Y.C. Yu, S.X. Cai, F.Y. Zhao, M. Arai, J. Catal. 269 (2010) 131.
[17] Y.F. Hao, R.X. Liu, X.C. Meng, H.Y. Cheng, F.Y. Zhao, J. Mol. Catal. A: Chem. 335 (2011) 183.
[18] X.C. Meng, H.Y. Cheng, S. Fujita, Y.C. Yu, F.Y. Zhao, M. Arai, Green Chem. 13 (2011) 570.
[19] X.D. Wang, M.H. Liang, H.Q. Liu, Y. Wang, J. Mol. Catal. A: Chem. 273 (2007) 160.
[20] M.H. Liang, X.D. Wang, H.Q. Liu, H.C. Liu, Y. Wang, J. Catal. 255 (2008) 335.
[21] A. Corma, P. Serna, P. Concepcion, J.J. Calvino, J. Am. Chem. Soc. 130 (2008) 8748.
[22] M. Takasaki, Y. Motoyama, K. Higashi, S.H. Yoon, I. Mochida, H. Nagashima, Org. Lett. 10 (2008) 1601.
[23] X.D. Wang, M.H. Liang, J.L. Zhang, Y. Wang, Curr. Org. Chem. 11 (2007) 299.
[24] Y. Wang, J.W. Ren, K. Deng, L.L. Gui, Y.Q. Tang, Chem. Mater. 12 (2000) 1622.
[25] C. Bock, C. Paquet, M. Couillard, G.A. Botton, B.R. MacDougall, J. Am. Chem. Soc. 126 (2004) 8028.
[26] Q. Wang, H.Y. Cheng, R.X. Liu, J.M. Hao, Y.C. Yu, F.Y. Zhao, Green Chem. 12 (2010) 1417.
[27] M.C. Biesinger, B.P. Payne, A.P. Grosvenor, L.W.M. Lau, A.R. Gerson, R.S. Smart, Appl. Surf. Sci. 257 (2011) 2717.
[28] J. Yang, H.W. Liu, W.N. Martens, R.L. Frost, J. Phys. Chem. C 114 (2010) 111.
[29] D.A.H. Cunningham, W. Vogel, M. Haruta, Catal. Lett. 63 (1999) 43.
[30] M. Olea, M. Tada, Y. Iwasawa, J. Catal. 248 (2007) 60.
[31] L.Q. Liu, B.T. Qiao, Y.B. Ma, J. Zhang, Y.Q. Deng, Dalton Trans. (2008) 2542.
[32] L.Q. Liu, B.T. Qiao, Z.J. Chen, J. Zhang, Y.Q. Deng, Chem. Commun. (2009) 653.
[33] L. Spiegler, N.J. Woodbury, US 3703,865.
[34] A.J. Dietzler, T.R. Keil, US 3067,253.
[35] M. Boudart, G. Djega-Mariadasson, in: Kinetics of Heterogeneous Catalytic Reactions, Princeton University Press, Princeton, NJ, 1984, p. 157.
[36] G.M. Schwab, Discuss. Faraday Soc. 8 (1950) 166.
[37] G.L. Haller, D.E. Resasco, Adv. Catal. 36 (1989) 173.